

Research Article

The TiN Content Computer Prediction Based on ANN and AR Model

¹Ma Chunyang, ¹Ding Junjie, ²Ning Yumei and ³Chu Dianqing

¹School of Mechanical Science and Engineering, Northeast Petroleum University, Daqing 163318, China

²School of computer science and technology, Xidian University, Xi'an 710071, China

³No. 4 Oil Production Plant, Petrochina Daqing Oilfield, Daqing 163000, China

Abstract: Artificial Neural Network (ANN) and autoregressive model (AR model) of nano TiN particles content in Ni-TiN composite coating was established by the method of time series analysis. In this paper, we want to seek for the TiN content computer prediction in Ni-TiN composite coatings by using ANN and AR model. The trend of the nano TiN particles content variation was forecasted with the AR model, and the prediction value and experimental test results were compared. The XRD patterns were investigated using X-ray Diffraction (XRD). The results show the number of the neuron in hidden layers is 10, and the optimal epoch is 3740. The ANN and AR model can forecast the nano TiN particles content in Ni-TiN composite coating. And the average deviation is about 5.2884%. The average grain size for Ni and TiN is approximately 52.85 and 39.13 nm, respectively.

Keywords: AR model, Ni-TiN composite coating, particles content

INTRODUCTION

Nano composite coatings are coatings which formed by components with characteristic dimensionality as nanometer size (1-100 nm) setting in different matrixes, and own better mechanical performances such as higher hardness, wear resistance and corrosion resistance (Borkar and Harimkar, 2011; Xiang *et al.*, 2011; Xia *et al.*, 2012; Zhou *et al.*, 2004; Baumann *et al.*, 2011; Jitputti *et al.*, 1995). The microhardness and wear resistance were affected by particles content in composite layer (Feng *et al.*, 2005; Sen *et al.*, 2010; Heidari *et al.*, 2010; Aruna *et al.*, 2007; Low *et al.*, 2006). However, the effect factors of particles content in composite coatings are the electrolyte composition, temperature, and plating conditions (such as current density, pH value, and stirring method), *et al.* And it is very difficult to predict the content of solid particles in composites accurately (Fustes *et al.*, 2008; Bund and Thiemig, 2007; Slimen *et al.*, 2011).

In this study, ANN was used to deal with the collected data of nano TiN particles in the composite coating. And AR model was used to forecast the trend of the nano TiN particles content variation and compare the prediction value with experimental test results.

ARTIFICIAL NEURAL NETWORK (ANN)

The original appearance for the Artificial Neural Network came from examination of central nervous

systems and their neurons, dendrites, axons, and synapses, which constitute the processing elements of biological neural networks investigated by neuroscience. Artificial Neural Network (ANN) is the simple artificial nodes which connected together to form a network of nodes mimicking the biological neural networks. Currently, the ANN tends to refer mostly to neural network models employed in statistics, cognitive psychology and artificial intelligence. Figure 1 shows the framework of artificial neural network model, and it is made up of input layer, hidden layer and output layer.

In modern software implementations of artificial neural networks, the approach inspired by biology has been largely abandoned for a more practical approach based on statistics and signal processing. In some of these systems, neural networks or parts of neural networks (such as artificial neurons) are used as components in larger systems that combine both adaptive and non-adaptive elements. While the more general approach of such adaptive systems is more suitable for real-world problem solving, it has far less to do with the traditional artificial intelligence connectionist models. What they do have in common, however, is the principle of non-linear, distributed, parallel and local processing and adaptation. Historically, the use of neural networks models marked a paradigm shift in the late eighties from high-level (symbolic) artificial intelligence, characterized by expert systems with knowledge embodied in if-then rules, to low-level (sub-symbolic) machine learning,

Corresponding Author: Chun-yang Ma, School of Mechanical Science and Engineering, Northeast Petroleum University, Daqing, China

This work is licensed under a Creative Commons Attribution 4.0 International License (URL: <http://creativecommons.org/licenses/by/4.0/>).

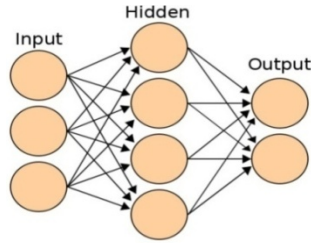


Fig. 1: Framework of artificial neural network model

characterized by knowledge embodied in the parameters of a dynamical system.

The word network in the term 'artificial neural network' refers to the inter-connections between the neurons in the different layers of each system. An example system has three layers. The first layer has input neurons, which send data via synapses to the second layer of neurons, and then via more synapses to the third layer of output neurons. More complex systems will have more layers of neurons with some having increased layers of input neurons and output neurons. The synapses store parameters called "weights" that manipulate the data in the calculations.

An ANN is typically defined by three types of parameters:

- The interconnection pattern between different layers of neurons
- The learning process for updating the weights of the interconnections
- The activation function that converts a neuron's weighted input to its output activation

Mathematically, a neuron's network function is defined as a composition of other functions, which can further be defined as a composition of other functions. This can be conveniently represented as a network structure, with arrows depicting the dependencies between variables. A widely used type of composition is the nonlinear weighted sum, where, where (commonly referred to as the activation function) is some predefined function, such as the hyperbolic tangent. It will be convenient for the following to refer to a collection of functions as simply a vector.

The first view is the functional view: the input is transformed into a 3-dimensional vector, which is then transformed into a 2-dimensional vector, which is finally transformed into. This view is most commonly encountered in the context of optimization. The second view is the probabilistic view: the random variable depends upon the random variable, which depends upon, which depends upon the random variable. This view is most commonly encountered in the context of graphical models. The two views are largely equivalent. In either case, for this particular network architecture, the components of individual layers are independent of each other (e.g., the components of are independent of each other given their input). This naturally enables a degree of parallelism in the implementation.

AR MODEL

AR model is the famous method and the most basic, the most practical application of time series model in time series analysis. It can not only observe linear correlation between data and forecasted the future trends of data, but also can research on related characteristics of the system in many sides. A model which depends only on the previous outputs of the system is called an Autoregressive Model (AR), while a model which depends only on the inputs to the system is called a Moving Average model (MA), and of course a model based on both inputs and outputs is an Autoregressive-Moving-Average model (ARMA). Note that by definition, the AR model has only poles while the MA model has only zeros. AR model of nano TiN particles content was established and nano TiN particles content in Ni-TiN composite coating was forecasted in this paper.

A difference equation model about $\{x_t\}$ can be fitted according to the timing method, while the observation time series $\{x_t\}$ is stable, meets the Normal Distribution and has zero-mean-value, and its formula as follows:

$$x_t - \varphi_1 x_{t-1} - \varphi_2 x_{t-2} - \dots - \varphi_n x_{t-n} = a_t - \theta_1 a_{t-1} - \theta_2 a_{t-2} - \dots - \theta_m a_{t-m} \quad (1)$$

where $\{a_t\}$ is a white noise series; $\varphi_1, \varphi_2, \varphi_3, \dots, \varphi_n$ are the auto-regressive parameters; $\theta_1, \theta_2, \theta_3, \dots, \theta_m$ are the parts of moving average; and n, m are the corresponding order.

An AR(1)-process is given by:

$$X_t = c + \varphi X_{t-1} + \varepsilon_t \quad (2)$$

where, ε_t is a white noise process with zero mean and variance σ_ε^2 . (Note: The subscript on φ_1 has been dropped.) The process is wide-sense stationary if $|\varphi| < 1$ since it is obtained as the output of a stable filter whose input is white noise. (If $\varphi = 1$ then X_t has infinite variance, and is therefore not wide sense stationary.) Consequently, assuming $|\varphi| < 1$, the mean $E(X_t)$ is identical for all values of t . If the mean is denoted by μ , it follows from:

$$E(X_t) = E(c) + \varphi E(X_{t-1}) + E(\varepsilon_t) \quad (3)$$

That

$$\mu = c + \varphi\mu + 0$$

And hence:

$$\mu = \frac{c}{1 - \varphi} \quad (4)$$

In particular, if $c=0$, then the mean is 0. The variance is:

$$\text{var}(X_t) = E(X_t^2) - \mu^2 = \frac{\sigma_\varepsilon^2}{1 - \varphi^2} \quad (5)$$

where σ_ε is the standard deviation of ε_t . This can be shown by noting that:

$$\text{var}(X_t) = \varphi^2 \text{var}(X_{t-1}) + \sigma^2 \quad (6)$$

And then the quantity above is a stable fixed point of this relation.

The autocovariance is given by:

$$B_n = E(X_{t+n} X_t) - \mu^2 = \frac{\sigma_\varepsilon^2}{1 - \varphi^2} \varphi^{|n|} \quad (7)$$

It can be seen that the autocovariance function decays with a decay time (also called time constant) of $\tau = -\frac{1}{\ln(\varphi)}$ [to see this, write $B_n = K\varphi^{|n|}$ where K is independent of n . Then note that $\varphi^{|n|} = e^{|n|\ln\varphi}$ and match this to the exponential decay law $e^{t\ln/\tau}$].

The spectral density function is the Fourier transform of the autocovariance function. In discrete terms this will be the discrete-time Fourier transform:

$$\Phi(\omega) = \frac{1}{\sqrt{2\pi}} \sum_{n=-\infty}^{\infty} B_n e^{-i\omega n} = \frac{1}{\sqrt{2\pi}} \left(\frac{\sigma_\varepsilon^2}{1 + \varphi^2 - 2\varphi \cos(\omega)} \right) \quad (8)$$

This expression is periodic due to the discrete nature of the X_j , which is manifested as the cosine term in the denominator. If we assume that the sampling time ($\Delta t = 1$) is much smaller than the decay time (τ), then we can use a continuum approximation to B_n :

$$B(t) \approx \frac{\sigma_\varepsilon^2}{1 - \varphi^2} \varphi^{|t|} \quad (9)$$

Which yields a Lorentzian profile for the spectral density:

$$\Phi(\omega) = \frac{1}{\sqrt{2\pi}} \frac{\sigma_\varepsilon^2}{1 - \varphi^2} \frac{\gamma}{\pi(\gamma^2 + \omega^2)} \quad (10)$$

where, $\gamma = 1/\tau$ is the angular frequency associated with the decay time τ .

An alternative expression for X_t can be derived by first substituting $c + \varphi X_{t-2} + \varepsilon_{t-1}$ for X_{t-1} in the defining equation. Continuing this process N times yields:

$$X_t = c \sum_{k=0}^{N-1} \varphi^k + \varphi^N X_{t-N} + \sum_{k=0}^{N-1} \varphi^k \varepsilon_{t-k}$$

For N approaching infinity φ^N will approach zero and:

$$X_t = \frac{c}{1 - \varphi} + \sum_{k=0}^{\infty} \varphi^k \varepsilon_{t-k} \quad (11)$$

It is seen that X_t is white noise convolved with the φ^k kernel plus the constant mean. If the white noise ε_t is a Gaussian process then X_t is also a Gaussian process. In other cases, the central limit theorem indicates that X_t will be approximately normally distributed when φ is close to one.

The above equations (the Yule-Walker equations) provide several routes to estimating the parameters of an AR (p) model, by replacing the theoretical covariance with estimated values. Some of these variants can be described as follows:

Here each of these terms is estimated separately, using conventional estimates. There are different ways of doing this and the choice between these affects the properties of the estimation scheme. For example, negative estimates of the variance can be produced by some choices.

Formulation as a least squares regression problem in which an ordinary least squares prediction problem is constructed, basing prediction of values of X_t on the p previous values of the same series. This can be thought of as a forward-prediction scheme. The normal equations for this problem can be seen to correspond to an approximation of the matrix form of the Yule-Walker equations in which each appearance of an autocovariance of the same lag is replaced by a slightly different estimate.

Formulation as an extended form of ordinary least squares prediction problem. Here two sets of prediction equations are combined into a single estimation scheme and a single set of normal equations. One set is the set of forward-prediction equations and the other is a corresponding set of backward prediction equations, relating to the backward representation of the AR model:

$$X_t = c + \sum_{i=1}^p \varphi_i X_{t+i} + \varepsilon_t^* \quad (12)$$

Here predicted values of X_t would be based on the p future values of the same series. These ways of estimating the AR parameters is due to Burg, and call the Burg method: Burg and later authors called these particular estimates "maximum entropy estimates", but the reasoning behind this applies to the use of any set of estimated AR parameters. Compared to the estimation scheme using only the forward prediction equations, different estimates of the autocovariances are produced, and the estimates have different stability properties. Burg estimates are particularly associated with maximum entropy spectral estimation.

Other possible approaches to estimation include maximum likelihood estimation. Two distinct variants of maximum likelihood are available: in one (broadly equivalent to the forward prediction least squares scheme) the likelihood function considered is that corresponding to the conditional distribution of later values in the series given the initial p values in the series; in the second, the likelihood function considered is that corresponding to the unconditional joint distribution of all the values in the observed series. Substantial differences in the results of these approaches can occur if the observed series is short, or if the process is close to non-stationarity.

The experiment was finished in School of Mechanical Science and Engineering, Northeast Petroleum University from October 2011 to April 2012.

RESULTS AND DISCUSSION

ANN was used to deal with the collected data of nano TiN particles in the composite coating. Based on the principle of AR model prediction, nano TiN particles content in Ni-TiN composite coating was forecasted by the established AR model. Measured values and predictive values of nano TiN composite particles in Ni-TiN composite coating were compared.

Collection data: The data of nano TiN composite particles in the composite coating were collected by atomic absorption spectrophotometer. The data (100 samples) were sorted according to the order of test pieces, and was used as a time-series data sequence of the AR model. As shown in Fig. 2. Ninety-four data were used to established AR model and the other six data as a test data. Table 1 presents the relation between the number of the neuron in hidden layers and the training epochs. From Table 1, the number of the neuron in hidden layers is 10, and the optimal epoch is 3740.

Forecasted results of AR model: AR model was determined according to the optimal order and the corresponding estimated parameters which calculated above. According to the Eq.(1)-(12), the value of the nano TiN particles content in composite coating was forecasted by the AR model. The sample approximation curve of nano TiN particles content in composite coating was drawn through AR model was shown in Fig. 3. Predictive value and the six tested value were compared in order to verify the applicability of the model. The predicted value of the first step forward and actual value was shown in Fig. 4.

Figure 4 shows that predicted value of the first step forward and actual value of nano TiN particles content in Ni-TiN composite coating was comparatively similar. And the average deviation is about 5.2884%.

Table 1: Relation between the number of the neuron in hidden layers and the training epochs

Number of the neuron	Epochs
4	10000
5	10000
6	10000
7	9952
8	5897
9	4915
10	3740
11	8576
12	10000
13	10000

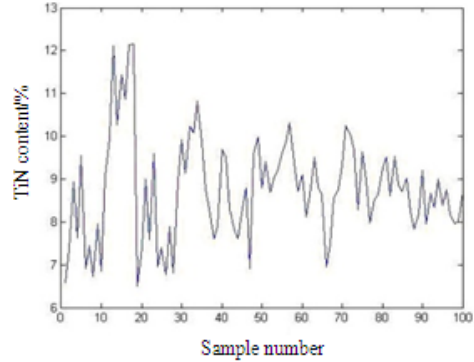


Fig. 2: Data series of nano TiN particles content

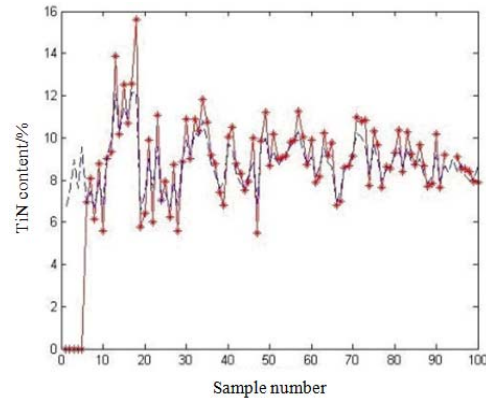


Fig. 3: Sample approximation curve of nano TiN particles content in composite coating

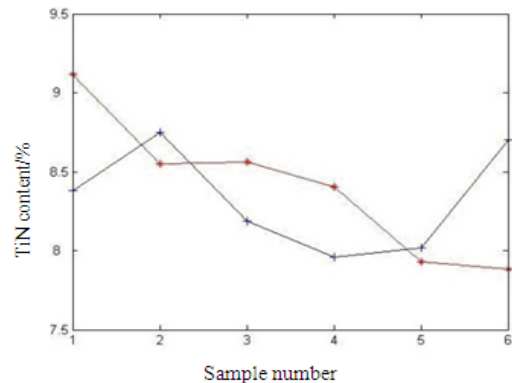


Fig. 4: Comparison between predicted value of and actual value of the TiN content

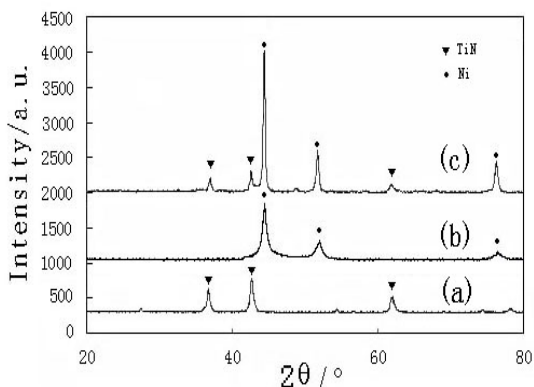


Fig. 5: XRD patterns of the TiN powder and coatings. (a) TiN powder, (b) Ni coating and (c) Ni-TiN coating

Composition analysis: Figure 5 presents XRD patterns of the TiN powder, Ni coating and Ni-TiN coating, which reveal the presence of TiN in the Ni-TiN coating. For Ni, the diffraction peaks at 44.82°, 52.21° and 76.77° correspond to (1 1 1), (2 0 0) and (2 2 0). For TiN, the diffraction peaks at 36.66°, 42.60° and 61.81° correspond to (1 1 1), (2 0 0) and (2 2 0). According to the XRD data, the average grain size for Ni and TiN calculated using Scherrer equation is approximately 52.85 and 39.13 nm, respectively.

CONCLUSION

Artificial Neural Network model (ANN) and AR model of nano TiN particles content in Ni-TiN composite coating was established by the method of time series analysis.

- ANN indicates that the number of the neuron in hidden layers is 10, and the optimal epoch is 3740.
- AR model can forecast the TiN content in Ni-TiN composite coatings. And the average deviation is about 5.2884%.
- XRD result demonstrates that the average grain size for Ni and TiN calculated is approximately 52.85 and 39.13 nm, respectively.

ACKNOWLEDGMENT

The authors gratefully acknowledge the National Natural Science Foundation of China (Grant 51101027) and National key technology support program (2012BAH28F03).

REFERENCES

Aruna, S.T., V.K. William Grips, V.S. Ezhil and K.S. Rajam, 2007. Studies on electrodeposited nickel-yttria doped ceria composite coatings. *J. Appl. Electrochem.*, 37(9): 991-1000.

Baumann, S.O., M.J. Elser, M. Auer, J. Bernardi and O. Diwald, 2011. Solid-solid interface formation in TiO₂ nanoparticle networks. *Langmuir*, 27(5): 1946-1953.

Borkar, T. and S. Harimkar, 2011. Microstructure and wear behaviour of pulse electrodeposited Ni-CNT composite coatings. *Surf. Eng.*, 27(7): 524-529.

Bund, A. and D. Thiemig, 2007. Influence of bath composition and pH on the electrocodeposition of alumina nanoparticles and nickel. *Surf. Coat. Technol.*, 201(16-17): 7092-7099.

Feng, X., J. Zhai and L. Jiang, 2005. The fabrication and switchable super hydrophobicity of TiO₂ nanorod films. *Angew. Chem-Ger Edit. I*, 117(32): 5245-5248.

Fustes, J., A. Gomes and M.I.P. Silva, 2008. Electrodeposition of Zn-TiO₂ nanocomposite films-effect of bath composition. *J. Solid State Electrochem.*, 12(11): 1435-1443.

Heidari, G., H. Tavakoli and S.M. Mousavi Khoie, 2010. Nano SiC-Nickel composite coatings from a sulfamat bath using direct current and pulsed direct current. *J. Mater. Eng. Perform.*, 19(8): 1183-1188.

Jitputti, J., Y. Suzuki and S. Yoshikawa, 1995. Synthesis of TiO₂ nanowires and their photocatalytic activity for hydrogen evolution. *Catal. Commun.*, 9(6): 1265-1271.

Low, C.T.J., R.G.A. Wills and F.C. Walsh, 2006. Electrodeposition of composite coatings containing nanoparticles in a metal deposit. *Surf. Coat. Technol.*, 201(1-2): 371-383.

Sen, R.J, S. Bhattacharya, S.H. Das and K.B. Das, 2010. Effect of surfactant on the co-electrodeposition of the nano-sized ceria particle in the nickel matrix. *J. Alloy. Compd.*, 489(2): 650-658.

Slimen, H., A. Houas and J.P. Nogier, 2011. Elaboration of stable anatase TiO₂ through activated carbon addition with high photocatalytic activity under visible light. *J. Photoch. Photobio. A*, 221(10): 13-21.

Xia, F.F., C. Liu, C.H. Ma, D.Q. Chu and L. Miao, 2012. Preparation and corrosion behavior of electrodeposited Ni-TiN composite coatings. *Int. J. Refract. Met. H.*, 35: 295-299.

Xiang, Q.J., J.G. Yu and M. Jaroniec, 2011. Enhanced photo-catalytic H₂-production activity of grapheme-modified titanic nanosheets. *Nanoscale*, 3: 3670-3678.

Zhou, W.Y., S.Q. Tang, L. Wan, K. Wei and D.Y. Li, 2004. Preparation of nano-TiO₂ photocatalyst by hydrolyzation-precipitation method with metatitanic acid as the precursor. *J. Mater. Sci.*, 39(3): 1139-1141.